

To Cite:

Zakaria AS, Khalial MG, Zahran AM, Ahmed MM, Alqalshy E.
Therapeutic effects of paclitaxel and nivolumab on cancer stem cells of
experimentally induced oral squamous cell carcinoma. Medical Science
2022; 26:ms425e2405.
doi: <https://doi.org/10.54905/disssi/v26i128/ms425e2405>

Authors' Affiliation:

¹Assistant lecturer, Oral and Dental Pathology department, Faculty of
Dental Medicine, (Boys), Al-Azhar University, Assiut, Egypt
²Assistant Professor, Department of Oral and Dental Pathology, Faculty
of Dental Medicine, (Boys), Al-Azhar University, Assiut, Egypt
³Professor, Department of Clinical pathology, South Egypt Cancer
Institute, Assiut University, Assiut, Egypt
⁴Professor, and head of Oral and Dental Pathology department, Faculty
of Dental Medicine, (Boys), Al-Azhar University, Cairo, Egypt
⁵Lecturer, Oral and Dental Pathology department, Faculty of Dental
Medicine, (Boys), Al-Azhar University, Cairo, Egypt

***Corresponding author**

Assistant lecturer, Oral and Dental Pathology department, Faculty of
Dental Medicine, (Boys), Al-Azhar University,
Assiut, Egypt
Email: ahmedsamirzakaria85@gmail.com

Peer-Review History

Received: 18 July 2022
Reviewed & Revised: 24/July/2022 to 17/October/2022
Accepted: 20 October 2022
Published: 24 October 2022

Peer-review Method

External peer-review was done through double-blind method.

URL: <https://www.discoveryjournals.org/medicalscience>



This work is licensed under a Creative Commons Attribution 4.0
International License.

Therapeutic effects of paclitaxel and nivolumab on cancer stem cells of experimentally induced oral squamous cell carcinoma

**Ahmed Samir Zakaria^{1*}, Mohamed Gomma Khalial²,
Asmaa Mohamed Zahran³, Mohamed Mahmoud
Ahmed⁴, Emad Alqalshy⁵**

ABSTRACT

Purpose: The main objective of this research was directed to evaluate the therapeutic effect of paclitaxel and nivolumab on cancer stem cells (CSCs) of experimentally generated hamster buccal pouch (HBP) carcinoma. **Methods:** 50 hamsters were grouped into five groups. GI: animals left untreated. GII: animals were painted with 7, 12-dimethylbenz (a) anthracene (DMBA) thrice a week. GIII: following DMBA application, animals injected intraperitoneally (IP) with nivolumab on days 7, 10 and 13. GIV: animals were treated with paclitaxel (IP), twice a week and metformin (IP), thrice a week. GV: animals were receiving a combination of nivolumab, paclitaxel and metformin. Following euthanization, right pouches were surgically excised, bisected with one section fixed and processed for H&E and immunohistochemical (IHC) examinations, and other section of the fresh tissue was used for evaluation by flow cytometric (FCM). **Results:** Gross observation histopathological, and IHC changes were recorded. By FCM, CD44+/CD24- and CD44+/CD24+ were detected. The results indicated that the CD44+/CD24- cells percentage in GI, GII, GIII, GIV and GV were 0.005%, 1.33%, 0.25%, 0.26% and 0.17%, respectively. While the CD44+/CD24+ cells percentage in GI, GII, GIII, GIV and GV was 0.001%, 0.11%, 0.05%, 0.03% and 0.02%, respectively. Apoptosis of CSC, in GI, GII, GIII, GIV and GV was 26.5%, 1.7 %, 38.1 %, 23.2% and 53.6% respectively. Regarding apoptosis of all cancer cells, the percentage of apoptotic cells is 1.72%, 24.5%, 54.2%, 48.3 and 68.3%, respectively. **Conclusions:** Combination of paclitaxel and nivolumab has the capability to suppress tumor development and induction of apoptosis in both CSC oral squamous cell carcinoma (OSCC) and non-CSC OSCC.

Keywords: Cancer stem cells; HBP carcinoma; Paclitaxel; Nivolumab

1. INTRODUCTION

According to the World Health Organization (WHO), the sixth greatest cause of cancer-related mortality globally is oral squamous cell carcinoma (OSCC)

(Kathiresan et al., 2016). Despite recent advances in cancer detection and treatment; the overall five-year survival rate for OSCC has remained less than 50% throughout the preceding three decades (Kim et al., 2016). Cancer stem cells (CSCs) are self-renewal cells capable of cell division and generation of distinct cancer cell types. Unlike normal stem cells, CSCs within tumors may renew and produce a variety of cancer cell types. Specific surface indicators and self-renewing characteristics are involved in the origin and development of cancer, as well as metastasis, recurrence and medication resistance (Cheng et al., 2016; Al-Dosoki et al., 2021). In most solid tumors, the proportion of CSCs is less than one percent (Yokoi et al. 2019), while in osteosarcoma; the proportion is closer to one percent (Yu et al., 2016). While in colon cancer patients the proportion of CSCs may reach to about 2% (Todaro et al., 2007). On the other hand, when the tumor grows, this percentage can rise to as much as 30% (Iyer et al., 2013), and this rise is associated with treatment resistance.

Tumor-inducing CSCs are a common occurrence (Sancho et al., 2015). They have been found in number of malignancy, including solid tumors such as pancreatic, breast, head & neck cancer (HNC), colon, bladder, liver, and lung cancers (Cherciu et al., 2014; Dragu et al., 2015). Chemo- and radiotherapy resistance, cell cycle passivity, DNA repair capabilities, particular morphological alterations, and up regulation of drug efflux and detoxifying enzymes all play a role in CSCs' function in cancer relapse and metastasis (Yadav et al., 2019). Oral carcinogenesis generated by 7, 12-dimethylbenz (a) anthracene (DMBA) is the most extensively utilized model for studying oral carcinogenesis biochemical changes and the chemopreventive potential of natural and synthetic therapies (Nagini, 2009). An animal model commonly used to study the development of cancer in the mouth is the hamster buccal pouch (HBP). It is important to keep in mind that the hamster still has numerous distinct characteristics that must be considered when evaluating data from oral carcinogenesis research (Tanaka et al., 2011).

Nivolumab, a monoclonal antibody that targets programmed cell death1 (PD-1), was the first PD-1 inhibitor approved outside of Japan in July 2014 for the treatment of melanoma. The FDA awarded it expedited approval in 2014 for treatment in non-small-cell lung malignancies (NSCLCs), renal cell carcinoma, metastatic melanoma, Hodgkin lymphoma and HNC (Bellmunt et al., 2017). Paclitaxel is a naturally occurring tricyclic diterpenoid molecule obtained from the bark of *Taxus brevifolia*, a Pacific yew tree. To date, it is one of the most potent and commonly used natural anticancer medications (Zhu et al., 2019). Paclitaxel is an anti-cancer medication that specifically targets microtubules. Paclitaxel stimulates tubulin microtubule assembly and prevents microtubule dissociation, which inhibits mitosis, cell cycle progression, and development of malignant cells (Weaver, 2014). Treatment of breast, colorectal, HNC and bladder tumors with paclitaxel has been common during the past several decades (Chen et al., 2016).

As a first-line treatment for diabetes mellitus type 2, metformin an FDA-approved biguanide derivative, is administered (Dowling et al., 2011). Clinical trials have shown that the drug can lower the chance of developing variety of tumors, including prostate (Colquhoun et al., 2012), lung (Li et al., 2014), breast (Blandino et al., 2012), esophageal (Xu et al., 2013), colon cancer (Algire et al., 2010), and even melanoma (Niehr et al., 2011). Additionally, in combination with conventional chemotherapy and radiation metformin can be utilized as a sensitizer to combat cancer (Lengyel et al., 2015; Uehara et al., 2015). Differentiation cluster CD44 is a transmembrane glycoprotein of mesenchymal and neuroectodermal origin that is defined in a different cell types (Windt et al., 2011). Cellular adhesion (aggregation and migration), hyaluronate breakdown, and hyaluronic acid synthesis are all activities of CD44. CD44 was used to establish the appearance of OSCC CSCs and their function in tumor growth and metastasis (Sawant et al., 2016).

A cell surface protein CD24 resembles mucin in size and glycosylation. There is a high level of CD24 expression in human malignancies including breast, ovarian, prostate and bladder cancers. Metastasis is dependent on cell adhesion. This suggests that CD24 might be a critical marker for tumor prognosis and detection (Jaggupilli et al., 2012). The objective of this study was directed to evaluate the therapeutic effect of Paclitaxel and/or nivolumab on CSCs of experimentally induced HBP carcinoma.

2. MATERIALS AND METHODS

The Experimental animals used in the current study were golden Syrian hamsters. They were used as a model for carcinoma induction utilizing DMBA as chemical carcinogen. Then, nivolumab, paclitaxel treatment started by intraperitoneal injection (IP), were employed. After that, various investigations including haematoxylin and eosin (H&E) stain, immunohistochemical (IHC) staining utilizing CSC marker anti CD44 and CD24, detection of CSC apoptosis by flowcytometry (FCM) were done. These procedures were done in FCM Unit, Clinical Pathology Department, Assiut Cancer Institute, South Egypt, Assiut University. The study is part of a research work started on March 2021 and ended in March 2022.

Animals

Cairo University's animal house (Cairo, Egypt), provided us with 50 male Syrian hamsters, 5 weeks old and weighing 80-120g. With sawdust bedding and humidity levels of 30-40 percent, temperature of ($20 \pm 2^{\circ}\text{C}$), and 12 hours of light and darkness, the experimental animals were kept in normal cages.

Sample size

For the current investigation, an eighty percent power to identify the difference in means of 0.53 with an alpha level (two-tailed) of significance (0.05) at a 95 percent confidence interval is predicted by the research of (Duzgun et al., 2017). These results are "statistically significant" if the p value (two-tailed) is 0.05 or less in 80% of the study. The differences among means were declared "no significant" in the other 80% of the studies. GraphPad StatMate 2.00 was used to make this report.

Chemicals

Dissolved in paraffin oil, DMBA (0.5%) was acquired from (Sigma-Aldrich) business. The drug Nivolumab (BMS-936558, ONO-4538, or MDX1106, Bristol-Myers Squibb, Princeton, NJ, USA). To prepare nivolumab, it was dissolved in a solution of sodium chloride at a concentration of 0.9%. Bristol-Myers and Sigma Aldrich supplied paclitaxel and metformin, respectively (St. Louis, MO, USA). To prepare metformin, a solution of 1 percent normal saline sodium chloride was added directly into the drug.

Experimental design

Following a week of adaptation the animals were distributed randomly into five groups of ten hamsters in each group: GI (normal group) animals, were fed and watered only and served as negative controls (Velu et al., 2017). GII (DMBA) for 14 weeks the right HBP were painted three times weekly with a number 4 camel's hair brush with DMBA in liquid paraffin and served as positive controls (Vinoth and Kowsalya, 2018). GIII (nivolumab): animals, after termination of painting with DMBA for 14 weeks, injected (IP) with nivolumab by insulin syringe 200 μL per injection on days 7, 10 and 13. On day 22, animals' buccal pouch were excised (Sanmamed et al., 2015). GIV (Paclitaxel- metformin) animals injected (IP) with paclitaxel 20mg/kg twice a weekly for three weeks (Harada et al., 2014) and metformin also injected (IP) 10 mg/kg 3 time a week for 3 weeks (Qi et al., 2016). GV (Nivolumab - Paclitaxel - Metformin) after 14 weeks of painting with DMBA, animals were receiving a combination of nivolumab, paclitaxel and metformin using the same dosage and mode of administration as single treatments.

Investigations

After the end of the experiment, animals were euthanized and the HBP excised and divided into two specimens. One specimen was embedded into paraffin blocks for H&E and IHC examination after being preserved in 10% neutral buffered formalin. Other fresh tissue specimens were mechanically digested, suspended, and coupled with fluorophore-antibodies specific for the CSC surface marker and detect by (FACS).

IHC staining

In primary OSCC tissue samples, the CD44 and CD24 CSC markers were evaluated using IHC analysis. Using citrate-buffer antigen solution pH 6.0 at 95°C for 35 minutes, Slides were deparaffinized, rehydrated, and antigen retrieval was performed in a Steamer. It was then treated for 20 minutes at room temperature (RT) with Protein Block Serum-Free (Dako, Carpinteria, CA) to prevent subsequent agents from binding nonspecifically, and slices were incubated in 3 percent hydrogen peroxide for 20 minutes. A total of one hour was spent incubating the tissue slices with the primary anti-mouse CD44 and CD24 antibodies at room temperature. For 45 minutes at room temperature, tissue slices were exposed to a biotin-free peroxidase visualization system after washing. Finally, after applying and washing the DAB substrate-chromogen system (Dako) for 1 minute, the slides were counterstained with Meyer's haematoxylin.

Analysis of CSCs using FCM

OSCC dissociation using physical methods: In a 35-mm petri dish, the tumor mass is put with 3 mL of phosphate buffer saline solution (PBS). For removing blood and other debris, the tumor mass was thoroughly washed in PBS two or three times. A scalpel blade with a number 22 and tissue forceps were used to hold the specimen in place while the blade was used to scrape the specimen downward and away from the bulk of tumor. Strands of connective tissue fibers were separated and eliminated from the collection as tumor cells were broken up. For as long as possible, we scraped the dish until the specimen was too little to hold. A 5-ml disposable pipet was used to pump the tumor solution up and down for 3 to 5 minutes. The suspension was then poured into a 15-

ml conical tube. It became centrifuged for 2 minutes at 2500 rpm and 4°C with the remaining sample. After removing the solution, the cellular pellet was resuspended in PBS at a level sufficient for FACS analysis before being analyzed.

Detection of CSCs

In suitable volume the cellular pellet was suspended in PBS. 10 µl of phycoerythrin-labeled anti-mouse CD24 (PE-CD24) monoclonal antibody (clone G44-26; BD Biosciences, CA, USA), Allophycocyanin -labeled anti-mouse CD44 (APC-CD44) monoclonal antibody (clone M1/69; Elabscience Biotechnology, Texas, USA), annexin V (FITC) and propidium iodide (PI) were added to 100 µl of suspension sample. For 25 minutes at 4°C, the suspension was incubated with the antibodies and protected from light. In PBS the cells were resuspended, and 50000 cells acquired by the (FACSCanto) flow cytometer (BD Biosciences). Based on light scatters cells were first gated followed by positive gating of CD44+ CD24- , CD44+ CD24+ cells. Then CD44+ CD24- were further gated for analysis of apoptosis.

Apoptosis assays for cancer cells

Apoptosis Detection Kit with Annexin V-FITC/PI (Elabscience Biotechnology, Texas, USA). Cell suspensions were washed and resuspended in 100 L of annexin V-conjugate binding solution, which also included 10 L of FITC-conjugated annexin and 10 L of (PI). After 25 minutes, 400 L of the binding buffer was added. A FCM was used to examine the cells (BD FACSCalibur, San Jose, CA, USA).

Statistical analyses

The findings were presented as the mean ± standard deviation and the number of observations accompanying the results. SPSS version 17.0 for windows was used to run an ANOVA with one factor. If the p-value was less than 0.05, it was considered significant; otherwise, it was regarded non-significant. If the p-value was higher than 0.05, it was considered highly significant.

3. RESULTS

Gross observation

GI (Normal group), Animals didn't show any gross changes, with healthy and active behavior; and both buccal pouches' length was about 5 cm. The right HBP mucosa appears with flat and smooth surface without visible anomalies (Fig.1a). GII (DMBA treated group), animals revealed a bad smell and whitish debris coming out from their mouth. Marked perioral hair loss in all hamsters was noted up to the abdomen in some animals, significant body weight loss which may have been caused by poor food intake due to DMBA-induced inflammation in the oral cavity. The pouch depth began to decrease up to 2 cm and remained fixed until end of the experiment. Multiple elevated nodules were found on the right HBP mucosa. A white membrane and roughened granular surface were found on the pouch mucosa (Fig.1b). GIII (Nivolumab treated group), the general health of the animals had significantly improved. The pouches length has increased approximately 3 cm. Compared to animals treated with DMBA, the right HBP mucosa revealed remarkable decrease in size and number of exophytic masses (Fig.1c). GIV (Paclitaxel and metformin treated group), the right HBP mucosa presented with visible rough granular surface. Visible oral tumor incidences were detected, and some tumors gradually decreased in size and number of nodules with absence of erosive and bleeding area (Fig.1d). GV (Nivolumab, Paclitaxel and metformin treated group), Animals showed marked improvement in the general health. The right HBP mucosa showed small size nodules with mucosa presented granularity and erythema, exophytic tumor mass decreased in size significantly, when compared to animals treated with DMBA without ulceration and bleeding (Fig.1e).

Histopathological results

In GI, H&E stain revealed that the lining epithelium of HBP mucosa is extremely thin, with 3-4 cell of keratinized stratified squamous epithelium. Thin epithelium with polyhedral prickle cell and granular cell layer with thin keratohyaline granules were observed in the epithelium. With a tiny layer of keratin, the epithelial tissue was covered. There was a layer of striated muscle fibers in the submucosal tissue, as well as delicate and loose connective tissue (Fig. 1f). In GII, H&E staining revealed those 8 cases had well differentiated SCC, while two cases had moderate SCC. Malignant epithelial cells invaded the connective tissue of well-differentiated SCC. Invading epithelial cells manifested themselves as epithelial pearls or cell nests with keratin foci, or as loose and dispersed cells producing keratin. Tumor cells with pleomorphic, hyperchromatic nuclei showed an abnormal nuclear/cytoplasmic ratio (Fig.1g). In GIII six cases demonstrated an infiltration of malignant cells on the surface in the form of highly differentiated SCC, and four cases showed severe dysplasia, according to H&E stain (Fig.1h). In GIV seven cases showed superficial invasion of

tumor cells in the form of well-differentiated SCC, and three instances showed severe dysplasia, according to H&E staining results (Fig.1i). In GV, H&E stain indicated that, 4 cases exhibited superficial invasion of the cell nests in the form of well differentiated SCC and 6 cases exhibited severe epithelial dysplasia (Fig.1j).

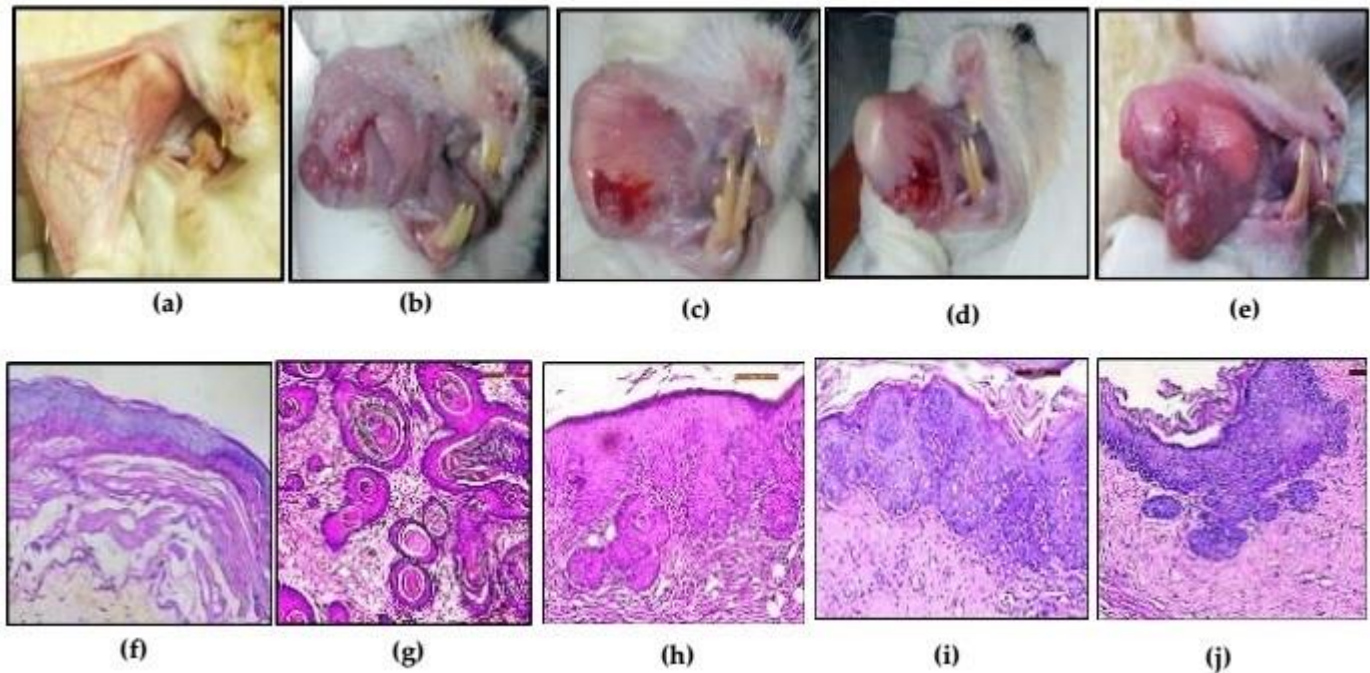


Figure 1 (a) Photograph of GI (normal) the right HBP mucosa appears pink in color with flat surface and no obvious abnormalities; (b) Photograph of GII (DMBA) revealing several exophytic papillary tumor masses encircled by hemorrhagic regions; (c) Photograph of GIII (nivolumab) demonstrating a minor size elevation without ulceration or hemorrhage; (d) Photograph of GIV (Paclitaxel and metformin) exhibited tiny size nodule; (e) Photograph of GV (Nivolumab, paclitaxel and metformin) demonstrating a significant reduction in the size of nodules and absence of ulceration and bleeding; (f) Photomicrograph of GI (normal) showing 2-4 cell thick keratinized stratified squamous epithelium. Thin epithelium with layers of polyhedral prickle cells and granule cell with fine keratohyaline granules (H&E stain X200); (g) Photomicrograph of GII (DMBA) presenting well differentiated SCC, malignant epithelial cells invaded into the connective tissue appeared as epithelial pearls or cell nests with keratin foci (H&E stain X200); (h) Photomicrograph of GIII (nivolumab) showing well differentiated SCC with early invasion of tumor cells (H&E stain X200); (i) Photomicrograph of GIV (Paclitaxel and metformin) demonstrating well differentiated SCC with superficial invasion of tumor cells (H&E stain X200); (j) Photomicrograph of GV (Nivolumab, paclitaxel and metformin) revealed well differentiated SCC with superficial invasion of malignant cells (H&E stain X200)

IHC results

In the GI, IHC staining revealed that CD44 predominantly stained in a membrane pattern, with a slight component of cytoplasmic staining and very infrequent nuclear staining. CD44 antigen was found as a brownish staining on the epithelial cells (35.3 percent) in the basal and suprabasal cells, which subsequently faded to reveal the superficial keratin layer in its negative state (Fig.2a). While CD24 staining was predominantly cytoplasmic, it was expressed with the highly differentiated upper layers of normal epithelium (0.3 percent) in contrast to basal layer (Fig.2b). In the GII, IHC staining revealed that CD44 antigen was localized to the basal and parabasal layers, as well as to the periphery cells of the tumor nests, as brownish membranous staining (65.5 percent). In addition to membranous staining, cytoplasmic labeling was also observed. (Fig.2c). While CD24 was highly expressed (68.6 percent) (Fig.2d).

SCC Immunopositivity to CD24 was extremely variable. Even within the same example, membranous and cytoplasmic immunostaining was detected in well-differentiated locations with pearl formation, and in tumor invasion sites devoid of keratinized cells respectively. CD44 antigen was found as a strong brownish membranous, cytoplasmic staining around the border and bulk of the tumor nests, with a weak staining into the keratin pearls (51.4 percent) in GIII (Fig.2e). While CD24 expressed positively in the cytoplasm and membrane compartments (32.4 percent) of all epithelial layers (Fig.2f). CD44 antigen was found as a strong brownish cytoplasmic membranous, staining in the basal and suprabasal cells of tumor nests (50.2 percent) by IHC staining (Fig.2g). While CD24 expressed abundantly in the cytoplasm, it was also detected in the membrane layer (33.3 percent) throughout the epithelial layers (Fig.2h) in GIV. CD44 antigen was found as a mild brownish membranous, cytoplasmic staining in the basal and

suparabasal cells of tumor nests (40.3 percent) in the GV group (Fig.2i). While CD24 expressed positively in the cytoplasm (10.5 percent) in all epithelial layers (Fig.2j).

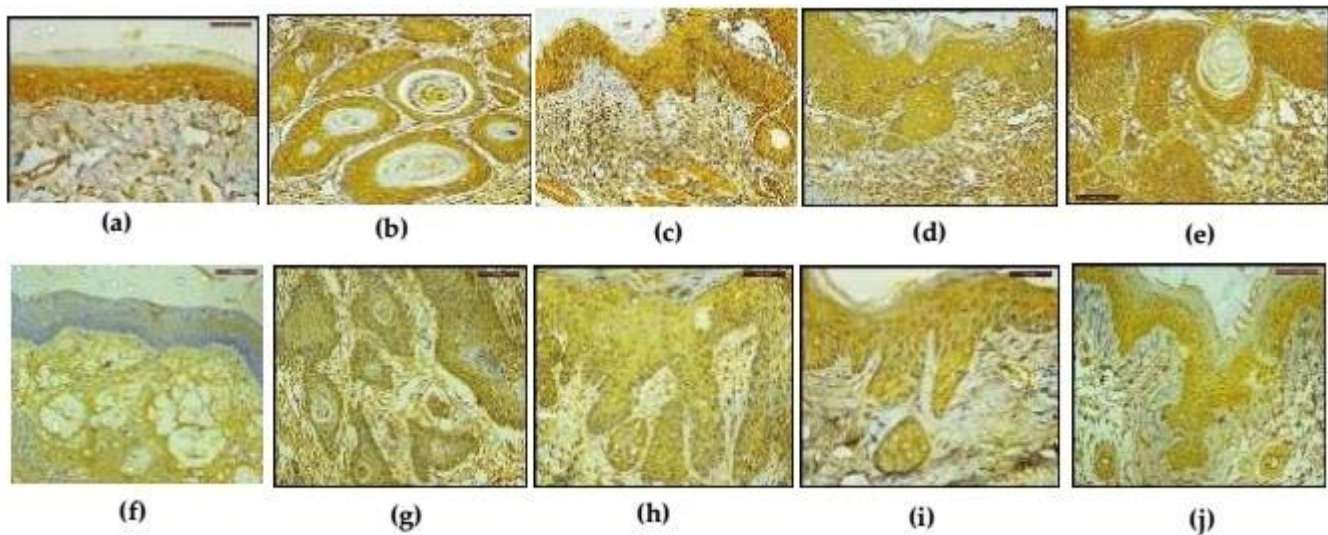


Figure 2 (a)IHC expression of CD44 in GI (normal) revealed positive membranous expression in basal layer and parabasal cells; (b) IHC expression of CD24 in GI (normal) showing positive membranous and cytoplasmic expression in superficial layer and negative in the basal layer; (c) IHC expression of CD44 in GII (DMBA group) showing positive membranous and cytoplasmic expression in tumor island; (d)IHC expression of CD24 in GII (DMBA group) showing positive membranous and cytoplasmic expression in superficial layer; (e)IHC expression of CD44 in GIII (Nivolumab group) showing positive membranous-cytoplasmic expression throughout the epithelial layers and invading tumor cells; (f) IHC expression of CD24 in GIII showing positive membranous-cytoplasmic expression throughout the epithelial layers and invading tumor cells; (g) IHC expression of CD44 in GIV (Paclitaxel group) showing positive membranous-cytoplasmic expression throughout the epithelial layers and invading tumor cells; (h) IHC expression of CD24 in GIV showing positive membranous-cytoplasmic expression throughout the epithelial layers and invading tumor cells; (i) IHC expression of CD44 in GV (Nivolumab and Paclitaxel group) showing positive membranous-cytoplasmic expression throughout the epithelial layers and invading tumor cells; (j) IHC expression of CD24 in GIV showing positive membranous-cytoplasmic expression throughout the epithelial layers and invading tumor cells.

Statistically there was highly significant difference between GI and GII regarding to CD44 and CD24 (P-value < 0.001).There was no statistically significant difference between GII, GIII and GIV regarding to CD44 (P-value = 0.076) (P-value = 0.054). There was statistically significant difference between GII and GV (P-value = 0.002) regarding to CD44. There was statistically highly significant difference between GII, GIII, GIV and GV regarding to CD24 (P-value < 0.001) (Fig. 3).

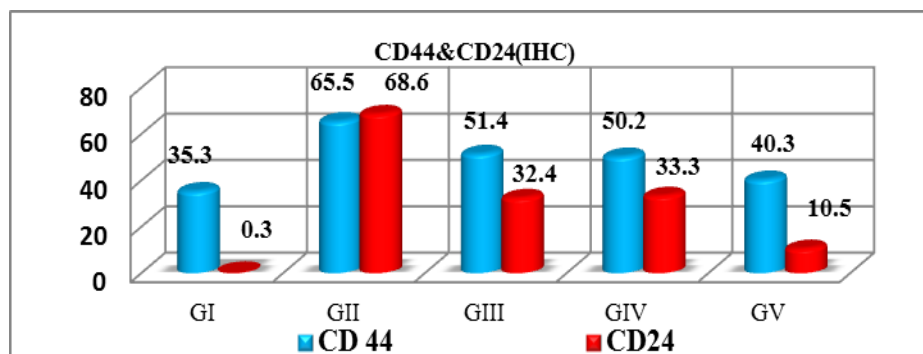


Figure 3 Bar chart representing mean results regard to CD44 and CD24

Identification of cancer stem cells

Two distinct phenotypic subpopulations of CD44+/CD24- and CD44+/CD24+ cells were identified using (FCM). The data revealed that the CD44+/CD24- cells percentage was 0.005 percent, 1.33 percent, 0.25 percent, 0.26 percent, and 0.17 percent in GI, GII, GIII, GIV, and GV, respectively. CD44+/CD24+ cells percentage was 0.001 percent, 0.11 percent, 0.05 percent, 0.03 percent, and 0.02 percent in GI, GII, GIII, GIV, and GV, respectively, as revealed in (Fig.4). Statistically there was a highly significant difference in CD44+/CD24- between GI, GII, GIII, and GIV (P-value 0.001). Additionally, there was a statistically significant difference in

CD44+/CD24- ratios among GI and GV (P-value = 0.008). While, there was a highly statistically significant differences in CD44+/CD24- ratios between GII, GIII, GIV, and GV (P-value 0.001) (Fig. 4). However, there is no statistically significant difference in CD44+/CD24- between GIII and GIV (P-value = 0.866). There was a statistically significant difference in CD44+/CD24- ratios between GIII and GV (P-value=0.041). There was a statistically significant difference in CD44+/CD24- across GIV and GV (P-value = 0.044).

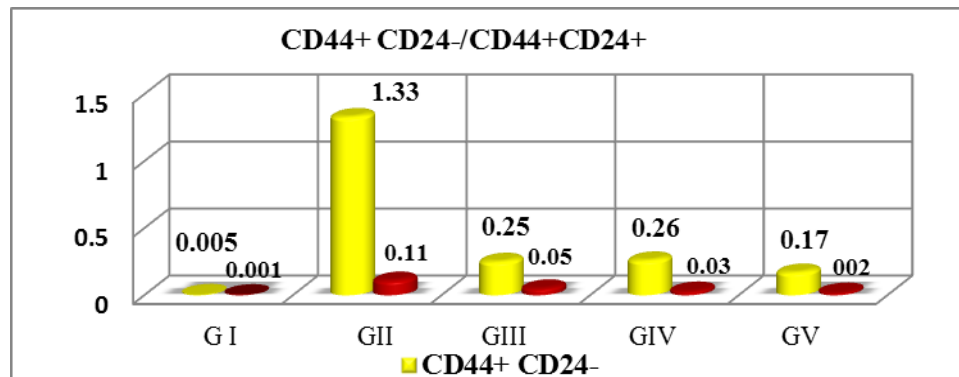


Figure 4 Bar chart showing mean results of CD44+/CD24-, CD44+/CD24+

Apoptosis results

The percentage of apoptotic CSC was 26.5%, 1.7 %, 38.1%, 23.2%, and 53.6% in GI, GII, GIII, GIV, and GV, respectively. There was a highly statistically significant difference in CSC apoptosis between GI, GII, and GV (P-value 0.001). However, no statistically significant difference in CSC apoptosis was seen among GI, GIII, and GIV (P-value = 0.06, 0.585, respectively). Statistically there was a highly significant difference in CSC apoptosis across GII, GIII, and GV (P-value 0.001). Additionally, there was a statistically significant difference between GII and GIV, GIII and GIV (P-value = 0.001) (p-value = 0.019) respectively, in terms of CSC apoptosis. There was significant difference between GIII and GV (P-value =0.013). There was a highly statistically significant difference (P-value 0.001) in CSC apoptosis between GIV and GV (Fig. 5) with regards to all cancer cells undergoing apoptosis. As indicated in (Figure 5), the percentages of apoptotic cells in GI, GII, GIII, GIV, and GV were 1.72 percent, 24.5 percent, 54.2 percent, 48.3 percent, and 68.3 percent, respectively. Statistically there was a highly significant difference in apoptosis of malignant cells among GI, GII, GIII, GIV, and GV (P-value 0.001). While, there was a highly statistically significant difference in apoptosis of all cancer cells between GII, GIII, GIV, and GV (P-value 0.001).

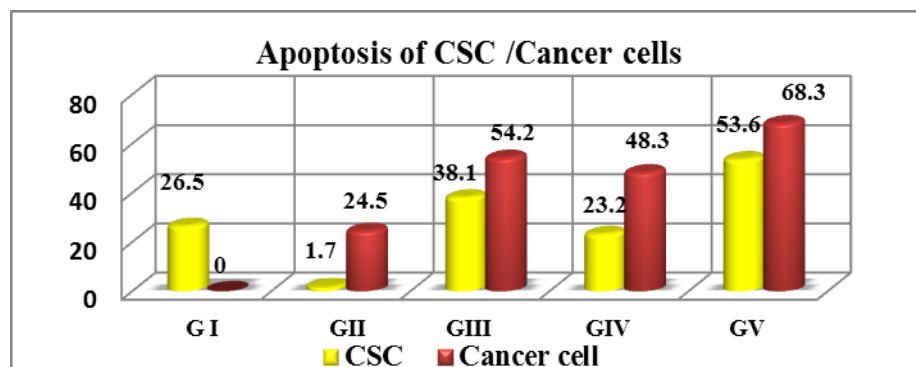


Figure 5 Bar chart illustrating mean of apoptosis of CSC and cancer cells

4. DISCUSSION

OSCC is among the most prevalent malignant cancers in humans, accounting for 2% of all cancers. Standard of living for OSCC patients improved, but the 5-year survival rate stays the same despite significant improvements in treatment methods, such as surgery, radiation, chemotherapeutic and multidisciplinary complete sequence therapy (Liu et al., 2021). The rapid growth of the (CSC) theory in recent years provides a new understanding of carcinogenesis. The CSC population possesses stem cell-like features, including as self-renewal and strong in vivo tumor formation and differentiation capacity, as well as multidrug and apoptotic resistance (Luo et al., 2020).

Gross results in the GI (normal group) demonstrated no abnormalities of the HBP in the present investigation. There were no skin outbreaks, and the hair seemed healthy. When they were sacrificed, all of the hamsters with normal histology had buccal pouches that were about 5 cm long. The results of this study are in accordance with those of other research that have made similar claims (Casto et al., 2013; El-Hossary et al., 2018). According to H&E staining, which revealed a normal two- to four-layer stratified squamous epithelium without rete ridges or a thick surface layer of keratin, this conclusion was confirmed. The results of this study are in line with those of (Grawish et al., 2010; Ezzat et al., 2017). This could be because the hamsters were not exposed to the carcinogenic substance, which could explain the results.

In the current study, GI (normal group), IHC staining showed a positive expression of CD44 in the basal and suprabasal cells with lacking expression in the corneal layers (mean= 35.3). IHC results of CD44 in the healthy oral epithelium were present as brownish membranous staining that was exclusive to epithelial cells. This observation might be attributed to that; Because CD44 is involved in the maintenance structure of epithelial as a whole through the homing of epithelial cells, this observation may be explained. A study by Kaza et al., (2018) found that CD44-positive generative cells of the epithelium could be targets for malignant transformation. On statistical evaluation, it was found that mean level of expression of CD44 in normal group in stratum basale was (mean= 35.3). This result is in agreement with other investigator (Godge et al., 2011).

CD24 expression was detected by (IHC) with a weak staining (mean= 0.3) rather than the expected stem basal layer, it was mostly connected with the upper, highly developed normal epithelium layers. CD24 has been linked to keratinocyte differentiation in previous studies (Abdul Majeed et al., 2013). Our results were consistent with research work done by (Kristiansen et al., 2003) who observed that ovarian cancer and colorectal carcinoma were reported to have significant CD24 expression, while normal tissue had low CD24 expression. In the current study, CD44⁺/CD24⁺ cells percentage in GI was 0.005 in the present study with regard to apoptosis of all specimen cells. In the untreated cells (normal control), 1.72% of the cells underwent apoptosis. This result in agreement with other investigator (Saleh et al., 2020).

In the present study, the gross observation findings in GII showed multiple exophytic masses of variable size surrounded by area of ulceration and bleeding. There is general debilitation of animals, significant reduction of the pouches' length, corresponding with results of studies using the same model (El-Mansy et al., 2017; El-Hossary et al., 2018). These findings are largely owing to the harmful effects of DMBA. Oral tumors of various grades formed in the research animals at various points in time. Mariadoss et al., (2013) observed that painting DMBA alone for fourteen weeks on the HBP resulted in 100 percent tumor growth, which is in keeping with our findings. These findings were in line with those of earlier research conducted by Kirshnakuwar et al., (2013); Rajasekaran et al., (2015). In contrast to the present study, Yang et al., (2006), and Hussein et al., (2018) reported that OSCC induced by DMBA was seen in the examined HBPs was 53.5%, 76.9% and 66.67% respectively. This mismatch may be due to the using of different type of carcinogenic agent or technique or using old hamsters rather than the young ones.

This finding reflected on H&E staining in which histologically, DMBA-induced HBP tumors were well to moderately differentiated SCC in the form of deeply invading islands of epithelium into the underlying connective tissues. Based on previous studies, this finding is in agreement with them (Manoharan et al., 2013). Because of the carcinogenic nature of DMBA, which is converted by phase I enzymes like cytochrome P450 to the carcinogenic dihydrodiol-epoxy derivative that damages DNA and causes mutation, this could be an explanation (Baldasquin-Caceres et al., 2014). The carcinogenesis stages (initiation, promotion, and progression) have been linked to ROS as well occur as a consequence the ROS-induced DNA damage, change in DNA, stimulation of proto-oncogenes, and deactivation of suppressor tumor genes, cancerous transformation can occur (Naveenkumar et al., 2013).

Tumor aggressiveness was found to be correlated with elevated levels of CD44 expression, according to the results of the current investigation. DMBA-painted hamsters showed a significant increase in CD44 optical density (mean = 65.5). Their findings were statistically significant when compared to those of the control animal's tissue samples (GI). Mirhashemi et al., (2020) found increased CD44 expression in OSCCs of higher grade and stage, which is in line with the findings of the current investigation. The results of Rautava et al., (2003), and Oliveira et al., (2014), proven that greater CD44 expression would raise the likelihood of malignancy. In addition to the membrane staining, cytoplasmic stain was also observed in the OSCC instances. The connection between CD44's cytoplasmic domain and cytoskeletal linking proteins like ezrin and ankyrin, which can promote cell mobility on hyaluronan, may be the cause of this. Accordingly, this supports the findings of other researchers (Kaza et al., 2018).

In contrast to the findings of the current investigation, studies by González-Moles et al., (2006), Godge et al., (2011) and Krump et al., (2013) indicated that CD44 expression decreased with increasing OSCC grades as contrasted to the typical oral mucosa. In addition, (Hema et al., 2014) found that the expression of CD44 by tumor cells in OSCC reduced considerably with grade. According to the findings, decreased CD44 expression in OSCC may be caused by diminished cell-cell or cell-matrix adhesion, resulting in cell separation. This is what the researchers concluded. Reduced expression of CD44 may therefore be a sign of tumor

invasion and high metastatic potential. It is possible that this shortening of CD44's role may be owing to an incorrect choice of the tissues being studied, which may have large areas of infection, resulting in false results in CD44 expression. It's also possible that differences in the procedures used to identify CD44 expression in tissue, such as western blotting and FCM evaluations, will lead to inconsistent results (Rajarajan et al., 2012).

CD24 expression in GII revealed that epithelial layers and infiltrating cancer cells of displayed high CD24 expression (mean = 68.6 percent), that indicated extremely significant increase in expression in comparison to GI (p value = 0.01). The staining of CD24 in the keratin pearls of connective tissue matched with the other results in that it was abundant (Kristiansen et al., 2003; Sano et al., 2009). Esophageal SCC cells express more CD24 than normal in areas where keratin pearls occur, as reported by Sano et al., (2009). OSCC had higher levels of CD24 and CD44 expression than normal tissues, according to a study by Abdul Majeed et al., (2013). CD24 over expression has been linked to tumor development by De Moraes et al., (2017) suggesting that CD24 could be used as a therapeutic target and diagnostic biomarker in (HNSCC).

In the current study, CD24 immunostaining revealed two distinct staining signals membranous and cytoplasmic immunoreactivity in OSCC, in invasive and advanced locations of malignancies respectively. A previous study's findings are corroborated by these ones (Sano et al., 2009). According to Weichert et al., (2005), the change from apical membrane CD24 localization to cytoplasmic CD24 localization in normal cells and well-differentiated tumor cells indicates that epithelial cells are undergoing a change toward an invasive phenotype. This resembles the well-known change of tumor cells from epithelial to mesenchymal, which is related with the onset of invasiveness. Adhesion of CD24 expressing tumor cells with platelets expressing P-selectin lead to an increase in the excretion of tumor cells from the blood circulation and facilitate their escape. Another mechanism is that the connection between CD24 and Siglec-10 limits macrophage phagocytosis, preventing tumors from being removed by phagocytosis, which enhances tumor immune evasion (Yin et al., 2020).

We found two distinct cell phenotypes in this study. In breast and prostate cancer, CD44+/CD24- cells have been shown to have CSC features by several investigations (Ma Li et al., 2014). The CD44+/CD24+ CSC phenotype has been found in pancreatic and colorectal cancers in various investigations (Yeung et al., 2010). A few studies have suggested that CD44+/CD24- may be the CSC phenotype in OSCC (Chen et al., 2009; Chiu et al., 2013). In the current study, CD44+/CD24- and CD44+/CD24+ cells percentage in GII were 1.33 % and 0.11% respectively. This is in accordance with the findings of a previous research work (Todorokiet al., 2016). Higher tumor-initiating, clonogenic, and drug-resistant CD44+/CD24- cells are found in HNSCC (Ghuwalewala et al., 2016). This confirms the findings of prior studies.

CD44+/CD24-expressing cells were found to be capable of forming tumors in immunodeficiency mice, while cells with other phenotypes were unable to produce tumors. CD44+/CD24+ cells, on the other hand, are more self-renewing than CD44/CD24- cells, according to Ortiz-Montero et al., (2018), Han et al., (2014), and Li et al., (2007). The ABC-B1 transporter is over expressed in CD44+/CD24+ cells and it is thought to be a factor in the development of cells that are resistant to many drugs. More "stemness" was found in cells with the CD44+/CD24+ subpopulation than in cells with the CD44+/CD24- subpopulation when Oct-4, Sox-2, and Lin28 were all upregulated. In addition, chemotherapeutic drugs were less effective against CD24+/CD44+ cells than against CD44+/CD24- cells. CSC or tumor starting cells in HNSCC may be represented by a unique CD44+/CD24+ subpopulation, according to these findings.

In the current study, the percentage of apoptotic CSCs in GII resulted in 1.7 % apoptosis. Due to CSC's ability to enhance Bcl-2 compared to Bax, the mitochondrial retention of cytochrome C was increased, and apoptotic cell death was reduced. It is in accordance with the findings of (Todoroki et al., 2016; Ghuwalewala et al., 2016). In CD44+/CD24+ cells, anti-apoptotic genes including Bcl-2 and CFLAR were shown to be highly robustly expressed using real-time PCR. The P value observed (p-value 0.001) showed a highly significant difference among GI and GII in terms of CSC apoptosis. Apoptosis of CSCs was detected in GII at a rate of 1.7%, based on the findings of the current investigation. Due to CSC's ability to increase Bcl-2 compared to Bax, the mitochondrial retention of cytochrome C was promoted, which lead to reduce in apoptotic cell death, according to this study's findings. Todoroki et al., (2016), and Ghuwalewala et al., (2016), all found the same thing. It was revealed that Bcl-2 and CFLAR were found to be elevated in the CD44+/CD24- cells utilizing real-time PCR tests. The P value observed showed a highly statistically significant difference between GI and GII (p-value 0.001).

In the present study, with regard to the apoptosis of all cancer cells of GII resulted in 24.5% apoptosis. These results are in agreement with other research work. There was highly statistical significant difference across GI and GII regarding to apoptosis of cancer cells the P value recorded (p-value < 0.001). This finding is in line with those of other study (Saleh et al., 2020). In the present study, GIII (Nivolumab treated group) gross observation of the right HBP showed marked improvement in the general health. H&E staining showed that only 6 animals exhibited well differentiated SCC and 4 animals exhibited sever dysplasia. These results may attribute to that; Nivolumab was able to reduce oral invasive lesions by inhibiting the PD-1 signal in a specific way. Anti-PD-1

treatment dramatically lowered the frequency of oral lesions in mice and delayed malignant development in a similar study Okazaki et al., (2007).

The microenvironment of low-grade dysplastic lesions increased significantly the recruitment of CD8+ and CD4+ T cells in response to PD-1 inhibition in the presence of these lesions. T cells cross-linking with PD-L1-expressing tumors is caused by the anti-PD-1 binding to the PD-1 expression on T cells, and this leads to the enhancement of the immune system and the release of various cytotoxic molecules, including interleukin-2(IL-2), interferon-gamma (IFN γ) and tumor necrosis factor-alpha (TNF- α), all of which lead to the death of tumor cells these results in accordance with other studies (Lee et al., 2014; Cai et al., 2019). Apoptosis from anti-PD-1+ T cells is only possible when T cells are also attaching to tumor cells that express the PD-L1 receptor. HNSCC patients with higher PD-L1 expression had a poorer prognosis than those with lower expression of PD-L1 (Pardoll, 2012; Manni et al., 2017).

In the current study, IHC expression of CD44 in GIII revealed strong positive membranous expression but the expression was in lower level than GII (mean= 51.4). The results showed no significantly difference expression compared to GII (P-value = 0.076). CD44 is expressed in the basal and suprabasal layers of OSCC tumors, as well as in the periphery of tumor nests. This is consistent with previous investigations (Lee et al., 2014; Barkal et al., 2019). According to Lee et al., (2014) blocking tumor-infiltrating lymphocytes (TILs) with anti-PD-L1 and anti-PD-1 antibodies partially restored interferon (IFN)- γ secretion by TILs incubated with CD44+ cells, indicating that the PD-L1-PD-1 signaling pathway is involved in part of CD44+ cells' immunosuppressive properties. CD24 expression was positive (mean= 32.4) and present throughout the epithelial layers, there was a highly significant results in comparison to GII (p- value < 0.001). This result is in accordance with that of other researchers (Lee et al., 2014; Barkal et al., 2019).

CD44+/CD24- and CD44+/CD24+ cells percentages in GIII were 0.25 %and 0.05%, respectively, in the current study. When compared to the GII, the fraction of CD44+/CD24- cells is lower. These findings are consistent with those of other researchers (Tada et al., 2020). The findings of Tada et al., (2020) demonstrate that nivolumab treatment induces an efficient anticancer immune response, allowing the migratory tumor cells (CTCs) to present the CSC phenotype due to lysis of non-CSC tumor cells. Although CSCs are known to be self-renewing and differentiating subpopulations (Nassar et al., 2016), immunological characterization of CSCs shows that CSCs can evade immune surveillance by having lower immunogenicity and inhibition of immunity than non-CSC counterparts (Codony-Servat et al., 2015; Clara et al., 2020).

In the present study, the percentage of apoptotic CSCs in GIII resulted in 38.1% apoptosis. Regarding to apoptosis of CSC there was highly significant difference among GII and GIII (P-value < 0.001). This result is in agreement with other study. Wang et al., (2017) observed that mice treated with anti-PD-1 had more T cell activation in oral lesions, which led in the production of granzyme B, which may help to promote apoptosis. In this study, GIII resulted in 54.2 % apoptosis of all cancer cells. In terms of apoptosis of all cancer cells, there was a statistically significant difference between GIII and GII (P-value 0.001). Other studies have come to the same conclusion. T cells activation mediates the immunoinhibition effects of anti-PD-1 antibodies, according to Okazaki T.,(2007) who found that PD-1 blocking accompanied the creation of the T cells effector, granzyme B, in invading cells and the triggering of apoptosis in epithelial cells of oral lesions.

In the present study, GIV (Paclitaxel and metformin treated group) gross observation of the right HBP mucosa revealed that tumors gradually decreased in number of nodules and absence of erosive and bleeding surfaces. This finding in same line with other study (Rocha et al., 2011; Harada et al., 2014; Badr El-Din et al., 2016). Rocha et al., (2011) revealed that a combination of paclitaxel and metformin inhibited tumor growth more efficiently than each medication alone in a xenograft model. This was supported by H&E staining, which revealed early invasion of malignant cells in the form of well differentiated SCC in seven patients and severe dysplasia in three others. These findings could be due to the fact that metformin can make animals more sensitive to DNA damaging chemicals (Taxol/chemotherapy), which is a mitotic inhibitor used in cancer chemotherapy that interferes with microtubule formation. The microtubule/paclitaxel complex that results has an effect on cell function, causing mitotic arrest, cell division inhibition, and eventually apoptosis (Lengyel et al., 2015). Furthermore, we can attribute metformin's ability to lower ROS levels to the fact that increased levels of ROS in cancer cells might drive cancer growth by activating HIF-1 (Kuo et al., 2019).

In the current work, IHC CD44 results for GIV (Paclitaxel and metformin group) demonstrated positive membranous and cytoplasmic expression, but at a lower level than GII. CD44 is seen in the basal and suprabasal layers, as well as around the periphery of tumor nests (mean=50.2). There is no statistically difference across GII and GIV (P-value = 0.054) regarding to CD44 expression. This is in line with the findings of earlier investigations (Iliopoulos et al. 2011), who found that metformin and paclitaxel act together to diminish both CSCs and non-stem cancer cells. IHC expression of CD24 showed positive expression (mean= 33.3) which present in the superficial layers. This result is in agreement with that of other investigator (Iliopoulos et al., 2011). According to Zhang et al., (2015), treatment with cisplatin alone or metformin only did not significantly reduced tumor

growth, the combination of both drugs effectively inhibited tumor proliferation for up to five weeks after discontinuation of the medication. CD44+CD177+ CSCs and EMT were dramatically suppressed by metformin in vivo. Combining medicines that attack both the ovarian CSC and non CSCs is the most effective way to alleviate patient symptoms associated with tumor mass and eradicating the CSC population.

With regard to CD44+/CD24- and CD44+/CD24+ cells in GIV were found to be 0.26 % and 0.03%, respectively, in the current study. When compared to the GII, there is decline in the percentage of CD44+/CD24-positive cells. Other researchers have found the same thing (Chen et al., 2012; Cufi et al., 2012; Zhang et al., 2013). According to Iliopoulos et al., (2011) who showed that metformin and widely used chemotherapeutic agents including carboplatin, doxorubicin, and paclitaxel are highly effective in inhibiting tumor development and prevention of relapse in a wide range of cancer cell types when administered combined. Chemotherapeutic drug doxorubicin directly kills non-stem cancer cells (NSCCs), and this indirectly decreases the population of CSC by preventing the IL-6-mediated conversion. Metformin, on the other hand, appears to enhance the efficiency of standard chemotherapy when used in combination with decreased dosages of typical chemotherapeutic medicines.

Contrary to the results, Kuo et al., (2019) revealed that metformin does not directly attack HNSCC CSCs, but rather increases the presence of stem cell markers, indicating an increased ability to self-renew. Metformin has been noted to provide considerable protection from chemotherapy-induced cell death when used in conjunction with cisplatin. In addition metformin and chemotherapeutic drug were successful in reducing non-stem HNSCC cell populations. Metformin increases the activation of stem cell genes, most notably CD44 and BMI-1, which could explain the discrepancy. BMI-1 and CD44 are two of the most well-known CSC indicators, and both are essential for stem cell self-renewal.

In the current work, the percentage of apoptotic CSCs in GIV (Paclitaxel and metformin group) resulted in 23.2 % apoptosis. There was significant difference among GII and GIV regarding to apoptosis of CSC (P-value = 0.001). These result in the same line with other research work (Li et al., 2007). In the present study, cells of GIV (Paclitaxel and metformin group) resulted in 48.3 % apoptosis. Statistically there was highly significant difference between GII and GIV regarding to apoptosis of all cancer cells (P-value < 0.001). The findings were consistent with several in vitro reports in ovarian, breast, leukemia, prostate, pancreatic, lung cancer cells, Rogalska et al., (2014), and Gao et al., (2016), highlighting the apoptotic potential of metformin targeting different pathways of apoptosis. There was increase in expression of Bax and consequent decrease in Bcl-2 in most of cancer cells which was greatest with combination of metformin and paclitaxel. Hanna et al., (2012) hypothesized that the mTOR pathway and the apoptotic signaling cascade induced by microtubule destruction via paclitaxel, maybe through phosphorylation of the anti-apoptotic Bcl-2 protein, may be involved.

In the present study, GV (Nivolumab, Paclitaxel and Metformin treated group) animals showed significant enhancement, in the overall health. There was a significant elongation of the pouches reached to about 3.5cm after 3weeks of treatment and reduction in size of nodules. This finding reflected on H&E stain indicated that, 4 cases exhibited well differentiated SCC and 6 cases exhibited sever epithelial dysplasia. The lesions were well-differentiated, did not invade deeply into the underlying connective tissue, and often developed large amounts of keratin. Shi et al., (2012), Li et al., (2018), indicates that the conjunction of anti-PD-1 antibody and paclitaxel effectively inhibits tumor growth, and that the combined effect is much superior to the effect of either treatment alone.

Immune exhaustion is a process that occurs when ICIs like PD-1 present on CD8TILs interact with their ligands expressed on cancer cells, as shown in the study by Eikawa et al., (2015), who found that the mixture of metformin and anti-PD-1/PD-L1 suppressed the antitumor genic effect of CD8+ T tumor-infiltrating lymphocytes (CD8TILs). AMPK mTOR signaling blocks immune exhaustion in tumor tissues by targeting CD8TILs with metformin, which can override this suppressed state. As a result, the ability of CD8TILs to eliminate cancer cells from tumor tissues is increased (Kim et al., 2021). This finding could be explained by the synergistic effect of paclitaxel, metformin, and nivolumab, which increased intralesional T-cell activity and tumor clearance in vivo through PD-L1/PD-1 expression. Metformin can also promote T-cell activity by reducing the tumor microenvironment's hypoxia (Scharping et al., 2017).

Metformin appears to enhance the anticancer effects of anti-PD-1/PD-L1 inhibitors by lowering PD-L1 expression, as evidenced by a growing body of research. Cha et al., (2018) were the first to report that treatment with metformin in breast cancer was initially demonstrated to reduce endoplasmic reticulum-mediated degradation of cancer immune checkpoint receptor PD-L1. Researchers recently found that metformin stimulated Hippo signaling to reduce PD-L1 expression levels in colorectal cancer, therefore increasing immunotherapy's effectiveness against colorectal cancer. Increased cytotoxic capability of T cells and increased anticancer immunity can be achieved by inhibiting the negative regulation of immune function by PD-L1. It has been stated that the PD-1/PD-L1 antitumor effects may be enhanced by adding metformin, according to this research (Zhang et al., 2019).

On the other hand, metformin may elevate the expression of PD-L1 in wild-type NSCLC via the AMPK-LKB1 pathway, as demonstrated by Shen et al., (2020). If the immune checkpoint gene regulation discrepancy is linked to cancer cell types and

changes in the tumor suppressors and tumor microenvironment, it could have important implications. Drugs that disrupt microtubules can have direct implications on function of DC, in particular a powerful activation of DC maturation that promotes antitumor immunity (Kashyap et al., 2019). GV IHC staining showed that CD44 antigen was found as brownish membranous staining on the epithelial cells (mean=40.3) in the basal and suprabasal cells, showing negative staining in the corneal layers. These findings are in the same line with those of other studies (Lee et al., 2014). However, CD24 IHC expression was found throughout the tumor island to be positive cytoplasmic expression (mean=10.5). This attributed to that PD-1-PDL1 inhibition in vivo improves macrophage phagocytosis, inhibited tumor proliferation, and increases the lifespan of mice in mouse models of cancer in a macrophage-dependent manner, as demonstrated by Gordon et al., (2017).

As a part of this study, in GV the proportions of CD44+/CD24- and CD44+/CD24+ cells were calculated 0.17% and 0.02% respectively. There is a reduction in the percentage of CD44+/CD24- when compared to the GII. With regard to the percentage of apoptotic CSCs in GV (Nivolumab, Paclitaxel and Metformin group) resulted in 53.6% apoptosis. Statistically there was a highly significant difference among GII and GV regarding to apoptosis of CSC (P-value< 0.001). These findings, in consistence with Shi C et al., (2021) show that the paclitaxel combined with anti-PD-1 antibody can greatly suppress the growth of cervical cancer cells, while efficiently increasing apoptosis of cervical cancer cells. The PD-1 antibodies and PD-L1 ligand have the additional ability to stimulate T-cell activity, resulting in blockage of a high percentage of cells in the resting/growth 1 phase (G0/G1) phase, inhibition of cell growth, and increase cell death (Shi et al., 2021).

In GV, cells treated with (Nivolumab, Paclitaxel, and Metformin group) exhibited 68.3% apoptosis in the current study. In terms of apoptosis of all cancer cells, there was a statistically significant difference across GII and GV (P-value 0.001). Other research findings support these findings (Shi et al., 2021). Future research should focus on determining the best dosage and administration schedule for this combined medication or used the same drugs in combination with other drugs that having synergistic effect with the drugs used in the current study to be more effective against CSCs.

Our study presents some limitations that need to be highlighted. First, we are unable to isolate CSCs directly from the HBP due to the small size of tumor mass. Second, a simple immunostaining was employed to establish the CD44+/CD24- phenotype. Instead, double immunolabeling technique is required.

5. CONCLUSIONS

Finally, our findings suggested that a combined therapy of nivolumab and paclitaxel medicines for OSCC CSCs was a promising treatment choice. Immunotherapy is a viable treatment option for HNSCC. Patients with carcinoma have been proven to benefit from both single-drug and combination therapy in terms of reducing morbidity and extending survival. Furthermore, metformin appears to boost the sensitivity of CSCs to conventional chemotherapeutic agents when used in combination with regular chemotherapy medicines. CD44+ cells were unlikely to represent a pure population of CSCs, highlighting the necessity to evaluate it in conjunction with another marker.

Author Contributions

All authors contributed to the study conception and design. Conceptualization, Mohamed Mahmoud Ahmed, and Ahmed Samir; methodology, Mohamed Mahmoud Ahmed and Ahmed Samir; conducted experiment, Ahmed Samir and Emad Alqalshy; investigations, Mohamed Mahmoud Ahmed, Ahmed Samir, and Asmaa Zahran; data curation, Mohamed Mahmoud Ahmed, Ahmed Samir, and Asmaa Zahran, and Mohamed Gommakhial; writing and editing, Mohamed Mahmoud Ahmed, Ahmed Samir, and Asmaa Zahran, and Emad Alqalshy; All authors have read and agreed to the published version of the manuscript.

Ethics approval

The animal study protocol was approved by institutional Ethics Committee of faculty of dental medicine, Al-Azhar University, Egypt (protocol code 322/022019/125k and date of approval 19-2-2019).

Data Availability Statement

The data presented in this study are available on request from the corresponding author.

Informed Consent: Not applicable.

Funding

This study has not received any external funding.

Conflicts of interest

The authors declare that there are no conflicts of interests.

REFERENCES AND NOTES

1. Abdulmajeed A, Dalley A, Farah C. Putative cancer stem cell marker expression in oral epithelial dysplasia and squamous cell carcinoma. *J Oral Path Med* 2013; 42(10): 755-60.
2. Al-Dosoki MA, Abd-Alhafez AAA, Omar AMZ, Zouair MGA. Flow cytometric assessment of nivolumab and/or epigallocatechin-3-gallate on cancer stem cells of DMBA induced hamster buccal pouch carcinoma. *Medical Science* 2021; 25(118):3206-3221
3. Algire C, Amrein L, Zakikhani M, Panasci L, Pollak M. Metformin blocks the stimulative effect of a high-energy diet on colon carcinoma growth in vivo and is associated with reduced expression of fatty acid synthase. *J Endocr Relat Cancer* 2010; 17(2):351-60.
4. Badr El-Din N, Ali D, Alaa El-Dein M, Ghoneum M. Enhancing the apoptotic effect of a low dose of paclitaxel on tumor cells in mice by arabinoxylan rice bran (MGN-3/Biobran). *Nutrition and cancer* 2016; 68(6): 1010-20.
5. Baldasquin-Caceres B, Gomez-Garcia F, López-Jornet P, Castillo-Sanchez J, Vicente-Ortega V. Chemopreventive potential of phenolic compounds in oral carcinogenesis. *J Arch Oral Biol* 2014; 59(10): 1101-107.
6. Barkal A, Brewer R, Markovic M, Kowarsky M, Barkal S, Zaro B, Krishnan V, Hatakeyama J, Dorigo O, Barkal L and Weissman I. CD24 signalling through macrophage Siglec-10 is a target for cancer immunotherapy. *Nature* 2019; 572(7769):392-96.
7. Bellmunt J, Powles T, Vogelzang N. A review on the evolution of PD-1/PD-L1 immunotherapy for bladder cancer: the future is now. *Cancer treatment reviews* 2017; 54: 58-67.
8. Blandino G, Valerio M, Cioce M, Mori F, Casadei L, Pulito C, Sacconi A, Biagioni F, Cortese G, Galanti S, Manetti C. Metformin elicits anticancer effects through the sequential modulation of dicer and c-myc. *Nat Commun* 2012; 3(1):1-11.
9. Cai Y, Wang F, Liu Q, Li, Z, Li, D, Sun Z. A novel humanized anti-PD-1 monoclonal antibody potentiates therapy in oral squamous cell carcinoma. *Investig New Drugs* 2019; 37(5): 799-809.
10. Casto B, Knobloch T, Galioto R, Yu Z, Accurso B, Warner B. Chemoprevention of oral cancer by lyophilized strawberries. *Anticancer Res* 2013; 33(11): 4757-66.
11. Cha J, Yang W, Xia W, Wei Y, Chan L, Lim S, Li, Kim T, Chang S, Lee H, Hsu J. Metformin Promotes Antitumor Immunity via Endoplasmic-Reticulum-Associated Degradation of PDL1. *Mol Cell* 2018; 71(4): 606-20.
12. Chen G, Xu S, Renko K, Derwahl M. Metformin inhibits growth of thyroid carcinoma cells, suppresses self-renewal of derived cancer stem cells, and potentiates the effect of chemotherapeutic agents. *J Clin Endocrinol Metab* 2012; 97(4): 510-20.
13. Chen K, Shi W. Autophagy regulates resistance of non-small cell lung cancer cells to paclitaxel. *Tumor Biol* 2016; 37(8): 10539-44.
14. Chen Y, Chen Y, Hsu H, Tseng L, Huang P, Lu K, Chen D, Tai L, Yung M, Chang S, Ku H. Aldehyde dehydrogenase 1 is a putative marker for cancer stem cells in head and neck squamous cancer. *Biochem Biophys Res Commun* 2009; 385(3):307-13.
15. Cheng B, Yang G, Jiang R, Cheng Y, Yang H, Pei L, Qiu X. Cancer stem cell markers predict a poor prognosis in renal cell carcinoma: a metaanalysis. *Oncotarget* 2016; 7(40): 65862-75.
16. Cherciu I, Bărbălan A, Pirici D, Mărgăritescu C, Săftoiu A. Stem cells, colorectal cancer and cancer stem cell markers correlations. *Curr Health Sci J* 2014; 40(3):153-61.
17. Chiu C, Lee L, Li Y, Chen Y, Lu Y, Li Y, Wang H, Chang J, Cheng A. Grp78 as a therapeutic target for refractory head neck cancer with CD24- CD44+ stemness phenotype. *Cancer gene therapy* 2013; 20(11): 606-615.
18. Clara JA, Monge C, Yang Y, Takebe N. Targeting signalling pathways and the immune microenvironment of cancer stem cells—A clinical update. *Nature Rev Clin Oncol* 2020;17(4): 204-32.
19. Codony-Servat J, Rosell R. Cancer stem cells and immunoresistance: clinical implications and solutions. *Translational lung cancer res* 2015; 4(6):689-703.
20. Colquhoun A, Venier N, Vandersluis A, Besla R, Sugar L, Kiss A, Fleshner N, Pollak M, Klotz L, Venkateswaran V. Metformin enhances the antiproliferative and apoptotic effect of bicalutamide in prostate cancer. *Prostate Cancer Prostatic Diseases* 2012; 15(4):346-52.
21. Cufi S, Corominas-Faja B, Vazquez-Martin A, Oliveras-Ferreros C, Dorca J, Bosch-Barrera J, Martin-Castillo B, Menendez J. Metformin-induced preferential killing of

- breast cancer initiating CD44+CD24- cells is sufficient to overcome primary resistance to trastuzumab in HER2+ human breast cancer xenografts. *Oncotarget* 2012; 3(4): 395-8.
22. De Moraes F, Lourenço S, Ianez R, de Sousa E, da Conceição Silva M, Damascena A, Kowalski L, Soares F, Coutinho-Camillo C. Expression of stem cell markers in oral cavity and oropharynx squamous cell carcinoma. *Oral Surg Oral Med Oral Pathol Oral Radiol* 2017; 123(1): 113-22.
23. Dowling RJ, Goodwin PJ, Stambolic V. Understanding the benefit of metformin use in cancer treatment. *BMC med* 2011; 9(1):1-6.
24. Drag D, Necul L, Bleotu C, Diaconu C, Chivu-Economescu M. Therapies targeting cancer stem cells: current trends and future challenges. *World J Stem Cells* 2015; (7):1185-201.
25. Duzgun O, Sarici I, Gokcay S, Ates K, Yilmaz M. Effects of nivolumab in peritoneal carcinomatosis of malign melanoma in mouse model. *Acta Cirúrgica Brasileira* 2017; 32(12): 1006-12.
26. Eikawa S, Nishida M, Mizukami S, Yamazaki C, Nakayama E, Uono H. Immune-mediated antitumor effect by type 2 diabetes drug, metformin. *J Proc Natl Acad Sci USA* 2015; 112(6): 1809-14.
27. El-hossary W, Hegazy E, EL-Mansy M. Topical chemopreventive effect of thymoquinone versus thymoquinone loaded on gold nanoparticles on dmba-induced hamster buccal pouch carcinogenesis (immunohistochemical study). *Egy dent J* 2018; 64(3): 3523-33.
28. El-Mansy MN, Hassan MM, El-Nour A, Kholoud M, El-Hosary WH. Treatment of oral squamous cell carcinoma using thymoquinone loaded on gold nanoparticles. *Suez Canal Univ Med J* 2017; 20(1):11-9.
29. Ezzat S, Abuelkhair M, Mourad M, Helal M, Grawish M. Effects of aqueous cinnamon extract on chemically-induced carcinoma of hamster cheek pouch mucosa. *Biochem Biophys Rep* 2017; 12, 72-78.
30. Gao Z, Liu Z, Bi M, Zhang J, Han Z, Han X, Wang H, Sun G, Liu H. Metformin induces apoptosis via a mitochondria-mediated pathway in human breast cancer cells in vitro. *Exp Ther Med J* 2016; 11(5): 1700-6.
31. Ghuwalewala S, Ghatak D, Das P, Dey S, Sarkar S, Alam, N, Panda C, Roychoudhury S. CD44 (high) CD24 (low) molecular signature determines the cancer stem cell and EMT phenotype in oral squamous cell carcinoma. *Stem Cell Res J* 2016; 16(2): 405-17.
32. Godge P, Poonja L. Quantitative assessment of expression of cell adhesion molecule (cd44) splice variants: CD44 standard (CD44s) and v5, v6 isoforms in oral leukoplakias: an immunohistochemical study. *Indian J Dent Res* 2011; 22(3): 493-99.
33. Gonzalez-Moles M, Bravo M, Ruiz-Avila I, Esteban F, Bascones-Martinez A, Gonzalez-Moles S. Adhesion molecule CD44 expression in non-tumor epithelium adjacent to tongue cancer. *J Oral Oncol* 2004; 40(3): 281-86.
34. Gordon S, Maute R, Dulken B, Hutter G, George B, McCracken M, et al. PD-1 expression by tumour-associated macrophages inhibits phagocytosis and tumor immunity. *J Nature* 2017; 545(7655): 495-99.
35. Grawish M, Zaher A, Gaafar A, Nasif W. Long-term effect of spirulina platensis extract on dmba-induced hamster buccal pouch carcinogenesis (Immunohistochemical Study). *J Med Oncol* 2010; 27(1): 20-28.
36. Han j, Fujisawa T, Husain S, Pur R. Identification and characterization of cancer stem cells in human head and neck squamous cell carcinoma. *BMC cancer* 2014; 14(1): 1-1.
37. Hanna R, Zhou C, Malloy K, Sun L, Zhong Y, Gehrig P. Metformin potentiates the effects of paclitaxel in endometrial cancer cells through inhibition of cell proliferation and modulation of the mTOR pathway. *J Gynecol oncol* 2012; 125(2): 458-69.
38. Harada K, Ferdous T, Kobayashi H, Ueyama Y. Paclitaxel in combination with cetuximab exerts antitumor effect by suppressing NF-κB activity in human oral squamous cell carcinoma cell lines. *J Int oncol* 2014; 45(6): 2439-45.
39. Hema K, Rao K, Devi H, Priya N, Smitha T, Sheethal H. Immunohistochemical study of CD44s expression in oral squamous cell carcinoma-its correlation with prognostic parameters. *J Oral Maxillofac Pathol* 2014; 18(2): 162-8.
40. Hussein A, El-Sheikh S, Darwish Z, Hussein K, Gaafar A. Effect of genistein and oxaliplatin on cancer stem cells in oral squamous cell carcinoma: an experimental study. *Alex Dent J* 2018; 43(1): 117-23.
41. Iliopoulos D, Hirsch HA, Struhl K. Metformin decreases the dose of chemotherapy for prolonging tumor remission in mouse xenografts involving multiple cancer cell types. *J Cancer Res* 2011; 71(9):3196-201.
42. Iyer A, Singh A, Ganta S, Amiji M. Role of integrated cancer nanomedicine in overcoming drug resistance. *J Adv Drug Deliv Rev* 2013; 65(13-14): 1784-802.
43. Jaggupilli, Appalaraju, Elkord, Eyad. Significance of CD44 and CD24 as cancer stem cell markers: an enduring ambiguity. *J Clin Devel Immunol* 2012; 2012:1-11.
44. Kashyap A, Fernandez-Rodriguez L, Zhao Y, Monaco G, Trefny M, Yoshida N, Martin K, Sharma A, Olieric N, Shah P, Stanczak M. GEF-H1 signaling upon microtubule destabilization is required for dendritic cell activation and specific anti-tumor responses. *J Cell Rep* 2019; 28(13): 3367-380.
45. Kathiresan S, Govindhan A. [6]-Shogaol, a novel chemopreventor in 7, 12-dimethylbenz [a] anthracene-

- induced hamster buccal pouch carcinogenesis. *Phytotherapy Res* 2016; 30(4):646-53.
46. Kaza S, Kantheti L, Poosarla C, Gontu S, Kattappagari K, Baddam V. A study on the expression of CD44 adhesion molecule in oral squamous cell carcinoma and its correlation with tumor histological grading. *J Orofacial Sci* 2018; 10(1): 42-49.
47. Kim J, Park Y, Roh J, Cho K, Choi S, Nam S, Kim S. Prognostic value of glucosylceramide synthase and P-glycoprotein expression in oral cavity cancer. *Int J Clin Oncol* 2016; (21):883-89.
48. Kim Y, Vagia E, Viveiros P, Kang CY, Lee JY, Gim G, Cho S, Choi H, Kim L, Park I, Choi J. Overcoming acquired resistance to PD-1 inhibitor with the addition of metformin in small cell lung cancer (SCLC). *J Immunol Immunother* 2020; 70(4): 961-65.
49. Krishnakumar N, Sulfikkarali NK, Manoharan S, Venkatachalam P. Raman spectroscopic investigation of the chemopreventive response of naringenin and its nanoparticles in DMBA-induced oral carcinogenesis. *Spectrochim Acta A Mol Biomol Spectrosc* 2013; 115: 648-53.
50. Kristiansen G, Schlüns K, Yongwei Y, Denkert C, Dietel M, Petersen I. CD24 is an independent prognostic marker of survival in nonsmall cell lung cancer patients. *Br J Cancer* 2003; 88(2):231-36.
51. Krump M, Ehrmann J. Differences in CD44s expression in HNSCC tumors of different areas within the oral cavity. *Biomed Pap* 2013; 157(4): 1-4.
52. Kuo S, Honda C, Li W, Honda T, Kim E, Altuna X, Abhold E, Wang-Rodriguez J, Ongkeko W. Metformin results in diametrically opposed effects by targeting non-stem cancer cells but protecting cancer stem cells in head and neck squamous cell carcinoma. *Int J Mol Sci* 2019; 20(1): 1-16.
53. Lee Y, Sunwoo J. PD-L1 is preferentially expressed on CD44+ tumor-initiating cells in head and neck squamous cell carcinoma. *J Immuno Ther Cance* 2014; 2(3):270-76.
54. Lengyel E, Litchfield L, Mitra A, Nieman K, Mukherjee A, Zhang, Johnson A, Bradaric M, Lee W, Romero I. Metformin inhibits ovarian cancer growth and increases sensitivity to paclitaxel in mouse models. *Am J Obstet Gynecol* 2015; 212(4):479:1-10.
55. Li C, Heidt D, Dalerba P, Burant C, Zhang L, Adsay V, Wicha M, Clarke M, Simeone DM. Identification of pancreatic cancer stem cells. *J Cancer Res* 2007; 67(3): 1030-37.
56. Li J, Qi C, Liu X, Li C, Chen J, Shi M. Fibulin-3 knockdown inhibits cervical cancer cell growth and metastasis in vitro and in vivo. *Sci Rep* 2018; 8(1):1-8.
57. Li L, Han R, Xiao H, Lin C, Wang Y, Liu H, Li K, Chen H, Sun F, Yang Z, Jiang J. Metformin sensitizes egfr-tyk-resistant human lung cancer cells in vitro and in vivo through inhibition of il-6 signaling and emt reversal. *J Clin Cancer Res* 2014; 20(10):2714-26.
58. Liu Z, Zhou W, Lin C, Wang X, Zhang X, Zhang Y, Yang R, Chen W, Cao W. Dysregulation of foxd2-as1 promotes cell proliferation and migration and predicts poor prognosis in oral squamous cell carcinoma: a study based on Tcga data. *Aging (Albany Ny)* 2021; 13(2): 2379- 96.
59. Luo W, Liu R, Bai Y, Kong X, Liu H, Wu H, Liu HC. Identification, characterization and microrna expression profiling of side population cells in human oral squamous cell carcinoma tca8113 cell lines. *J Mol Med Rep* 2020; 22(1): 286-96.
60. Ma F, Li H, Wang H, Shi X, Fan Y, Ding X, Lin C, Zhan Q, Qian H, Xu B. Enriched CD44+/CD24- population drives the aggressive phenotypes presented in triple-negative breast cancer (TNBC). *J Cancer Lett* 2014; 353(2): 153-59.
61. Mann J, Hoesli R, Michmerhuizen N, Devenport S, Ludwig M, Vandenberg T, Matovina C, Jawad N, Mierzwa M, Shuman A, Spector M. Surveilling the potential for precision medicine-driven PD-1/PD-L1-targeted therapy in HNSCC. *J Cancer* 2017; 8(3): 332-44.
62. Manoharan S, Wani S, Vasudevan K, Manimaran A, Prabhakar M, Karthikeyan S, Rajasekaran D. Saffron reduction of 7, 12-dimethylbenz [a] anthracene-induced hamster buccal pouch carcinogenesis. *Asian Pac J Cancer Prev* 2013; 14(2): 951-57.
63. Mariadoss A, Kathiresan S, Muthusamy R, Kathiresan S. Protective effects of [6]-paradol on histological lesions and immunohistochemical gene expression in DMBA induced hamster buccal pouch carcinogenesis. *Asian Pac J Cancer Prev* 2013; 14(15): 3123-9.
64. Mirhashemi M, Ghazi N, Saghravanian N, Taghipour A, Mohajertehran, F. Evaluation of CD24 and CD44 as cancer stem cell markers in squamous cell carcinoma and epithelial dysplasia of the oral cavity by q-RT-PCR. *J Dent Res* 2020; 17(3), 208- 12.
65. Nagini S. Of humans and hamsters: the hamster buccal pouch carcinogenesis model as a paradigm for oral oncogenesis and chemoprevention. *J Anticancer Agents Med Chem* 2009; 9(8): 843-52.
66. Nassar D, Blanpain C. Cancer stem cells: basic concepts and therapeutic implications. *Annu Rev Pathol: Mechanisms of Disease* 2016; 11: 47-76.
67. Naveenkumar C, Raghunandhakumar S, Asokkumar S, Devaki T. Baicalein abrogates reactive oxygen species (ros) mediated mitochondrial dysfunction during experimental pulmonary carcinogenesis in vivo. *Basic clinical pharmac toxic J* 2013; 112(4): 270-81.
68. Niehr F, von Euw E, Attar N, Guo D, Matsunaga D, Sazegar H, Ng C, Glaspy J, Recio J, Lo R, Mischel P. Combination therapy with vemurafenib (plx4032/rg7204) and metformin

- in melanoma cell lines with distinct driver mutations. *Transl Med J* 2011; 9(1):76.
69. Okazaki, T, Honjo T. PD-1 and PD-1 ligands: from discovery to clinical application. *Int Immunol J* 2007; 19(7): 813-24.
 70. Oliveira L, Castilho-Fernandes A, Oliveira-Costa J, Soares F, Zucoloto S, Ribeiro-Silva A. CD44+/CD133+ immunophenotype and matrix metalloproteinase-9: Influence on prognosis in early-stage oral squamous cell carcinoma. *J Head Neck* 2014; 36(12): 1718-26.
 71. Ortiz-Montero P, Liu-Bordes W, Londoño-Vallejo A, Vernot J. CD24 expression and stem-associated features define tumor cell heterogeneity and tumorigenic capacities in a model of carcinogenesis. *Cancer Manag Res J* 2018; 10: 5767-84.
 72. Pardoll DM. The blockade of immune checkpoints in cancer immunotherapy. *J Nat Rev Cancer* 2012; 12(4): 252-64.
 73. Qi X, Xu W, Xie J, Wang Y, Han S, Wei Z, Ni Y, Dong Y, Han W. Metformin sensitizes the response of oral squamous cell carcinoma to cisplatin treatment through inhibition of NF- κ B/HIF-1 α signal axis. *J Sci Rep* 2016; 6:35788.
 74. Rajarajan A, Stokes A, Bloor BK, Ceder R, Desai H, Grafström RC, Odell E. CD44 expression in oro-pharyngeal carcinoma tissues and cell lines. *PLoS One* 2012; 7(1): 28776-86.
 75. Rajasekaran D, Manoharan S, Prabhakar MM, Manimaran A. Enicostemma littorale prevents tumor formation in 7,12-dimethylbenz(a)anthracene-induced hamster buccal pouch carcinogenesis. *Hum Exp Toxicol* 2015; 34(9): 911-21.
 76. Rautava J, Soukka T, Inki P, Leimola-Virtanen R, Sa-Ioniemi I, Happonen R, Heikinheimo K. CD44v6 in developing, dysplastic and malignant oral epithelia. *Oral Oncol* 2003; 39(4): 373-79.
 77. Rocha G, Dias M, Ropelle E, Osório-Costa F, Rossato F, Vercesi A, Saad M, Carnevalheira J. Metformin amplifies chemotherapy-induced AMPK activation and antitumoral growth. *Clin Cancer Res* 2011; 17(12): 3993-4005.
 78. Rogalska A, Forma E, Ciesielski P, Bryś M, Krześlak A, Marczak A. Effect of metformin on apoptosis induction in ovarian cancer cells. *Prz Menopauzalny* 2014; 13(3): 155-61.
 79. Saleh M, Darwish Z, El Nouaem M, Mourad G, Ramadan O. Chemopreventive effect of green tea and curcumin in induced oral squamous cell carcinoma: an experimental study. *J Alex Dent J* 2020; 45(3): 74-80.
 80. Sancho P, Burgos-Ramos E, Tavera A, Kheir T, Jagust P, Schoenhals M, Barneda D, Sellers K, Campos-Olivas R, Graña O, Viera C. MYC/PGC-1 α balance determines the metabolic phenotype and plasticity of pancreatic cancer stem cells. *Cell Metab J* 2015; 22 (4): 590-605.
 81. Sanmamed M, Rodriguez I, Schalper K, Onate C, Azpilikueta A, Rodriguez-Ruiz M, Morales-Kastresana A, Labiano S, Pérez-Gracia J, Martín-Algarra S, Alfaro C. Nivolumab and urelumab enhance antitumor activity of human T lymphocytes engrafted in Rag2-/- IL2R γ null immunodeficient mice. *Can Res J* 2015; 75(17): 1-40.
 82. Sano A, Kato H, Sakurai S, Sakai M, Tanaka N, Inose T, Saito K, Sohda M, Nakajima M, Nakajima T, Kuwano H. CD24 expression is a novel prognostic factor in esophageal squamous cell carcinoma. *Ann Surg Oncol J* 2009; 16(2): 506-14.
 83. Sawant S, Gokulan R, Dongre H, Vaidya M, Chaukar D, Prabhaskar K, Ingle A, Joshi S, Dange P, Joshi S, Singh A. Prognostic role of Oct4, CD44 and c-Myc in radio-chemo-resistant oral cancer patients and their tumorigenic potential in immunodeficient mice. *J Clin Oral Investig* 2016; 20(1):43-56.
 84. Scharping N, Menk A, Whetstone R, Zeng X, Delgoffe G. Efficacy of PD-1 blockade is potentiated by metformin-induced reduction of tumor hypoxia. *Cancer Immunol Res* 2016; 5(1):9-16.
 85. Shen X, Zhao Y, Liu G, Zhou H, Fan J, Zhang L, Li Y, Wang Y, Liang J, Xu Z. Upregulation of programmed death ligand 1 by liver kinase B1 and its implication in programmed death 1 blockade therapy in non-small lung cancer. *J Life Sci* 2020; 256:117923.
 86. Shi C, Zhang G, Peng L, Zhang K. Effect of anti-programmed cell death protein-1 antibody combined with paclitaxel on cervical cancer via phosphoinositide 3-kinase/protein kinase b pathway in rats. *Indian J Pharm Sci* 2021; 83(4): 823-29.
 87. Tada H, Takahashi H, Iwakawa R, Nagata Y, Uchida M, Shino M, Ida S, Mito I, Matsuyama T, Chikamatsu K. Molecular phenotypes of circulating tumor cells and efficacy of nivolumab treatment in patients with head and neck squamous cell carcinoma. *Sci Rep* 2020;10(1): 1-8.
 88. Tanaka T, Tanaka M, Tanaka T. Oral carcinogenesis and oral cancer chemoprevention: A review. *J Pathol Res Int* 2011; 2011: 1-10.
 89. Todaro M, Alea M, Di Stefano A, Cammareri P, Vermeulen L, Iovino F, Tripodo C, Russo A, Gulotta G, Medema J, Stassi G. Colon cancer stem cells dictate tumor growth and resist cell death by production of interleukin-4. *Cell Stem Cell* 2007; 1 (4): 389-402.
 90. Todoroki K, Ogasawara S, Akiba J, Nakayama M, Naito Y, Seki N, Kusukawa J, Yano H. CD44v3+/CD24-cells possess cancer stem cell-like properties in human oral squamous cell carcinoma. *Int J Oncol* 2016; 48(1): 99-109.
 91. Uehara T, Mitsunashi A, Tsuruoka N, Shozu M. Metformin potentiates the anticancer effects of cisplatin under normoxic conditions in vitro. *J Oncol Rep* 2015; 33(2): 744-50.
 92. Velu P, Vinothkumar V, Babukumar S, Ramachandhiran D. Chemopreventive effect of syringic acid on 7, 12-

- dimethylbenz (a) anthracene induced hamster buccal pouch carcinogenesis. *Toxicol Mech Methods* 2017; 27(8): 631-40.
93. Vinoth A, Kowsalya R. Chemopreventive potential of vanillic acid against 7, 12-dimethylbenz (a) anthracene-induced hamster buccal pouch carcinogenesis. *J Cancer Res* 2018; 14(6):1285.
94. Wang J, Xie T, Wang B, William W, Heymach J, El-Naggar A, Myers J, Caulin C. PD-1 blockade prevents the development and progression of carcinogen-induced oral premalignant lesions. *Cancer Prev Res* 2017; 10(12):684-93.
95. Weaver BA. How Taxol/paclitaxel kills cancer cells. *J Mol Biol Cell* 2014; 25(18): 2677-81.
96. Weichert W, Denkert C, Burkhardt M, Gansukh T, Bellach J, Altevoigt P, Dietel M, Kristiansen G. Cytoplasmic CD24 expression in colorectal cancer independently correlates with shortened patient survival. *Clin Cancer Res* 2005; 11(18):6574-81.
97. Windt GJ, Schouten M, Zeerleder S, Florquin S, Poll T. CD44 is protective during hyperoxia-induced lung injury. *Am J Respir Cell Mol Biol* 2011; 44(3):377-83.
98. Xu Y, Lu S. Metformin inhibits esophagus cancer proliferation through upregulation of usp7. *J Cell Physiol Biochem* 2013; 32(5):1178-86.
99. Yadav A, Desai N. Cancer stem cells: acquisition, characteristics, therapeutic implications, targeting strategies and future prospects. *Stem Cell Rev Rep* 2019; 15(3):331-55.
100. Yang Y, Zhou Z, Ge J. Effect of genistein on DMBA-induced oral carcinogenesis in hamster. *Carcinogenesis* 2006; 27(3): 578-83.
101. Yeung T, Gandhi S, Wilding J, Muschel R, Bodmer W. Cancer stem cells from colorectal cancer-derived cell lines. *J Proc Natl Acad Sci USA* 2010; 107(8): 3722-27.
102. Yin S, Gao F. Molecular mechanism of tumor cell immune escape mediated by CD24/Siglec-10. *Front Immunol* 2020; 11: 1324:1-10.
103. Yokoi E, Mabuchi S, Shimura K, Komura N, Kozasa K, Kuroda H, Takahashi R, Sasano T, Kawano M, Matsumoto Y, Kodama M. Lurbinectin (PM01183), a selective inhibitor of active transcription, effectively eliminates both cancer cells and cancer stem cells in preclinical models of uterine cervical cancer. *Invest new drugs* 2019; 37(5): 818-27.
104. Yu L, Fan Z, Fang S, Yang J, Gao T, Simões B, Eyre R, Guo W, Clarke R. Cisplatin selects for stem-like cells in osteosarcoma by activating Notch signaling. *J Oncotarget* 2016; 7(22): 33055-68.
105. Zhang J, Zhang Q, Li Z, Zhou J, Du J. Metformin attenuates PD-L1 expression through activating Hippo signaling pathway in colorectal cancer cells. *Am J Trans Res* 2019; 11(11): 6965-76.
106. Zhang R, Zhang P, Wang H, Hou D, Li W, Xiao G, Li C. Inhibitory effects of metformin at low concentration on epithelial-mesenchymal transition of CD44 + CD117+ ovarian cancer stem cells. *Stem Cell Res Ther* 2015; 6(1): 1-12.
107. Zhang Y, Guan M, Zheng Z, Zhang Q, Gao F, Xue Y. Effects of metformin on CD133+ colorectal cancer cells in diabetic patients. *PLoS One* 2013; 8(11): 1-8.
108. Zhu L, Chen L. Progress in research on paclitaxel and tumor immunotherapy. *J Cell Mol Biol Lett* 2019; 24(1): 1-40.